Frustrated spin-$\frac{1}{2}$ Ising antiferromagnet on a square lattice in a transverse field

A. Bobák,[1,*] E. Jurčišinová,[2] M. Jurčišin,[1,2] and M. Žukovič[1]
[1]*Department of Theoretical Physics and Astrophysics, Faculty of Science, P. J. Šafárik University, Park Angelinum 9, 041 54 Košice, Slovak Republic*
[2]*Institute of Experimental Physics, SAS, Watsonova 47, 040 01 Košice, Slovak Republic*

(Received 16 November 2017; published 15 February 2018)

We investigate the phase transitions and tricritical behaviors of the frustrated Ising antiferromagnet with first- ($J_1 < 0$) and second- ($J_2 < 0$) nearest-neighbor interactions in a transverse field Ω on the square lattice using an effective-field theory with correlations based on a single-spin approximation. We have proposed a functional for the free energy to obtain the phase diagram in the $T - R$ ($R = J_2/|J_1|$) or $T - \Omega$ planes. It is shown that due to the transverse field the phase transition between ordered and disordered phases changes in the tricritical point (TCP) from the second order to the first order. The longitudinal and transverse magnetizations are also studied for selected values of R and Ω. In particular, the variation of TCP at the ground state in the three-dimensional space is constructed. For some special cases, values of the critical temperature and the critical transverse field have been determined analytically.

DOI: 10.1103/PhysRevE.97.022124

I. INTRODUCTION

The Ising model in a transverse field, introduced by de Gennes in the context of ferroelectric systems [1], is defined by the Hamiltonian

$$H = -\sum_{\langle i,j\rangle} J_{ij} S_{iz} S_{jz} - \Omega \sum_i S_{ix}, \tag{1}$$

where S_{ix} and S_{iz} are Pauli matrices at site i, Ω is the transverse field, and J_{ij} are Ising coupling constants which only depend on the distance between i and j sites. The classical Ising model is recovered in the case $\Omega = 0$. Thus starting from the classical Ising model, one can obtain its quantum version by including a transverse-field term.

This model Hamiltonian represents one of the simplest spin models in which a phase transition occurs for a finite value of the external field. Namely, in an infinite model system described by Eq. (1) at all temperatures there is an order with $\langle S_{ix}\rangle \neq 0$. At high temperatures S_{iz} components of a spin operator at site i are disordered, but below a transition temperature they order so that $\langle S_{iz}\rangle \neq 0$. As Ω increases from zero, the transition temperature falls from its value in the Ising model and reaches zero at a critical value Ω_c. For $\Omega > \Omega_c$ no transition occurs.

Thermodynamic properties of the model Hamiltonian (1) have been obtained exactly only for the one-dimensional lattice [2–5] and in order to study higher-dimensional lattices some sort of approximation has to be used, such as a simple molecular-field approach or various perturbation methods (see, e.g., Ref. [6]).

On the other hand, in recent years interest in frustrated magnetic systems is constantly growing due to the permanent appearance of new materials belonging to this class (see Ref. [7] for a recent review). The frustration arises in physical systems due to the lattice geometry or the presence of competing interactions and prevents the simultaneous minimization of all microscopic interactions. The best known example of a frustrated magnetic system is the antiferromagnetic Ising model on a triangular lattice [8,9]. On the square lattice, which is a bipartite one, the frustration can be achieved either if the number of antiferromagnetic couplings limited to nearest neighbors (nn) around any elementary plaquette is odd [10] (so-called "odd model") or including at least the next-nearest-neighbor (nnn) couplings in addition to the nn interactions. In the latter case the frustration effect may arise due to the competition between the antiferromagnetic nn and the nnn interactions J_1 and J_2, respectively. In particular, it has been found (see, e.g., Refs. [11,12]) that for the value of the frustration parameter $R \equiv J_2/|J_1| > -0.5$ the ground state is the Néel antiferromagnet (AF) and in the case of $R < -0.5$ the system orders in alternate ferromagnetic rows (columns) of opposite oriented spins (superantiferromagnet-SAF) [13] (see the schemes in Fig. 1). The critical point separating these two phases lies at $R = -0.5$, where the transition temperature is suppressed to zero.

It is generally accepted that the transition line between the SAF and paramagnetic (P) phases exhibits a tricritical point (TCP) at which the phase transition changes from second order to first order. Such behavior has been confirmed not only by approximate methods [14–17], but also by Monte Carlo studies [12,18–20]. As pointed out only recently [17] the TCP exhibits also the effective-field phase diagram between AF and P phases (see also Ref. [20]).

The aim of the present work is within the effective-field theory (EFT) to discuss the phase diagram of the frustrated spin-$\frac{1}{2}$ transverse Ising AF with nnn interactions on a square lattice. The theory to be adopted is based on the approximate Ising spin identity introduced in Ref. [21] for the single-spin cluster in a transverse field. In this approach all the single-site kinematic relations are correctly accounted for and

*andrej.bobak@upjs.sk

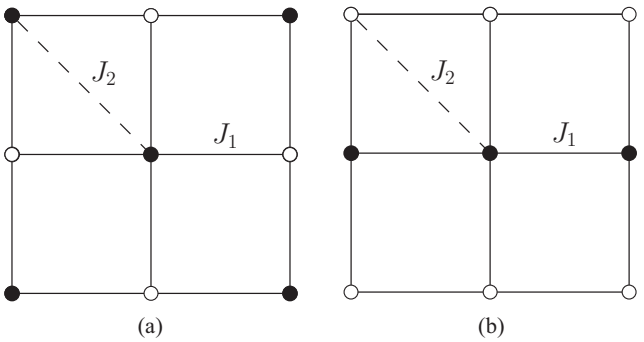

FIG. 1. Ground-state configurations of the $J_1 - J_2$ Ising model on the square lattice showing (a) antiferromagnetic and (b) superantiferromagnetic states for the single-spin cluster approximation. Two sublattices are marked by black and white circles.

only multispin correlation functions between various spins are decoupled. Hence, it will be interesting to consider the effect of the transverse field on the phase diagram of the frustrated quantum model. However, to provide any insight into the nature of possible first-order transition lines, we need to know the functional form of the free energy. For this reason we have proposed a free energy functional to analyze the first-order phase transition line between the ordered (AF or SAF) and disordered (P) phases. As far as we know such an investigation has not been made yet even in approximate theories.

In particular, we have found that the frustrated model with $\Omega = 0$ exhibits the TCP on the transition line between SAF and P phases, in agreement with previous approximate as well as Monte Carlo studies. In this case the TCP appears at $k_B T_t/|J_1| = 3.2207$ and $R_t = -1.3276$, and the first-order phase transition line shows a reentrant behavior at low temperatures (see the inset in Fig. 2). However, in contrast to the transition line between the AF and P phases, the first-order transition between the SAF and P phases terminates for $T \to 0$ at $R = -1.0$, which is inconsistent with the ground-state behavior of the model. This behavior is due to a lower symmetry of the SAF phase in comparison to the AF phase. Therefore, in this EFT, based on the single-spin cluster in a transverse field, we restrict ourselves to the AF phase which exists for $R > -0.5$. We believe that such a study can also contribute to the development of statistical mechanics and solid-state physics.

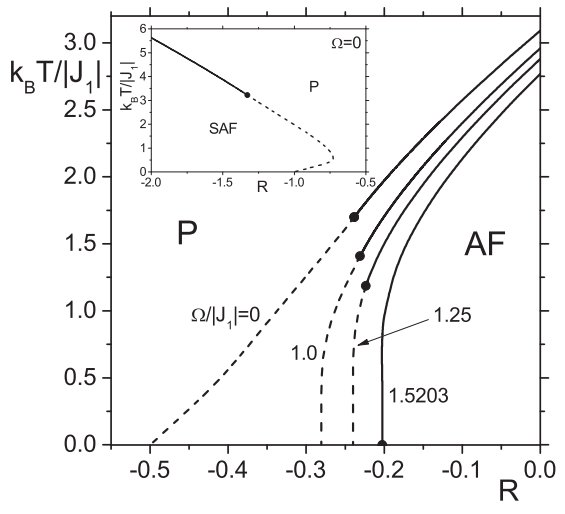

FIG. 2. Phase diagram in the coupling-temperature plane for the $J_1 - J_2$ Ising model on the square lattice based on the single-spin cluster, when values of the transverse field $\Omega/|J_1|$ are changed. Solid and dashed lines indicate second- and first-order transitions, respectively, while the black circles denote the position of a tricritical point. *AF* and *P* are the antiferromagnetic and paramagnetic phases, respectively. The inset shows phase diagram between the superantiferromagnetic (SAF) and P phases in the case of $\Omega/|J_1| = 0$ (see text).

II. THEORY

Generally, the Hamiltonian of the spin-$\frac{1}{2}$ Ising model with competing AF interactions between nn ($J_1 < 0$) and nnn ($J_2 < 0$) spins in the presence of a transverse field strength Ω is given by

$$H = -J_1 \sum_{\langle i,i_1 \rangle} S_{iz} S_{i_1 z} - J_2 \sum_{\langle i,i_2 \rangle} S_{iz} S_{i_2 z} - \Omega \sum_i S_{ix}, \qquad (2)$$

where the first summation is carried out only over nn pairs of spins, the second sum runs over nnn pairs of spins, and the last sum is taken over all sites.

The effective-field theory to be adopted is based on the approximate identity introduced in [21] for thermal average $\langle S_{i\alpha} \rangle$ ($\alpha = z$ or x) of a single spin

$$\langle S_{i\alpha} \rangle = \left\langle \frac{\mathrm{Tr}_{\{i\}}[S_{i\alpha} \exp(-\beta H_i)]}{\mathrm{Tr}_{\{i\}}[\exp(-\beta H_i)]} \right\rangle, \qquad (3)$$

where $\beta = 1/k_B T$ and the partial trace $\mathrm{Tr}_{\{i\}}$ is to be taken over the lattice site i. Here, H_i is that part of the Hamiltonian containing spin i, namely,

$$H_i = -E_i^z S_{iz} - \Omega S_{ix}, \qquad (4)$$

where the expression E_i^z for the model with first- and second-neighbor interactions reads

$$E_i^z = J_1 \sum_{i_1=1}^{z_1} S_{i_1 z} + J_2 \sum_{i_2=1}^{z_2} S_{i_2 z}, \qquad (5)$$

where z_1 and z_2 denote the numbers of nearest and next-nearest neighbors, respectively. In the limit of $\Omega = 0$, Eq. (3) reduces to the more widely known exact Callen-Suzuki relation [22,23] for the pure Ising model. However, for the transverse Ising model Eq. (3) is no longer exact and, as pointed out in Ref. [21], this equation is a reasonable approximation to the exact relation.

In order to diagonalize the form of Eq. (4) we use a rotation transformation,

$$\begin{aligned} S_{iz} &= \cos\Phi_i S_{iz'} - \sin\Phi_i S_{ix'}, \\ S_{ix} &= \sin\Phi_i S_{iz'} + \cos\Phi_i S_{ix'}, \end{aligned} \qquad (6)$$

where $\cos\Phi_i = E_i^z/E_i$, $\sin\Phi_i = \Omega/E_i$, and $E_i = [(E_i^z)^2 + \Omega^2]^{1/2}$. The diagonalization of this form leads to the following results for the longitudinal m_z and transverse m_x site magnetizations:

$$m_z \equiv \langle S_{iz} \rangle = \left\langle \frac{E_i^z}{E_i} \tanh(\beta E_i) \right\rangle, \qquad (7)$$

$$m_x \equiv \langle S_{ix} \rangle = \left\langle \frac{\Omega}{E_i} \tanh(\beta E_i) \right\rangle. \qquad (8)$$

To recast these equations in a more convenient form, the differential operator technique [24] and the Van der Waerden idenity for spin-$\frac{1}{2}$ operators may be employed to give

$$m_\alpha = \left\langle \prod_{i_1=1}^{z_1} [\cosh(J_1\nabla_y) + S_{i_1 z}\sinh(J_1\nabla_y)] \times \prod_{i_2=1}^{z_2} [\cosh(J_2\nabla_y) + S_{i_2 z}\sinh(J_2\nabla_y)] \right\rangle f_\alpha(y)|_{y=0}, \tag{9}$$

where $\nabla_y = \partial/\partial y$ is the differential operator and functions $f_\alpha(y)$, $(\alpha = z,x)$, are defined by

$$f_z(y) = \frac{y}{[y^2+\Omega^2]^{1/2}} \tanh[\beta(y^2+\Omega^2)^{1/2}], \tag{10}$$

$$f_x(y) = \frac{\Omega}{[y^2+\Omega^2]^{1/2}} \tanh[\beta(y^2+\Omega^2)^{1/2}]. \tag{11}$$

To proceed further, one now has to approximate the thermal multiple correlation functions occurring on the right-hand side of Eq. (9). The simplest approximation and the one most frequently adopted, is to decouple them according to

$$\langle S_{i_1} S_{k_1} \cdots S_{i_2}\rangle \approx \langle S_{i_1}\rangle\langle S_{k_1}\rangle \cdots \langle S_{i_2}\rangle, \tag{12}$$

where $i_1 \neq k_1 \neq \cdots \neq i_2$. It should be noted here that the present approximation neglects correlations between different spins but takes single-site kinematic relations, such as $S_{i_1}^{2n} = 1$ and $S_{i_1}^{2n+1} = S_{i_1}$ $(n = 1,2,\ldots)$, exactly into account through the Van der Waerden identity for spin-$\frac{1}{2}$ operators. Based on this approximation, Eq. (9), for the spin-$\frac{1}{2}$ Ising AF on a square lattice with $z_1 = 4$ and $z_2 = 4$ [see Fig. 1(a)], reduces to

$$m_{\alpha A} = [\cosh(J_1\nabla_y) + m_{zB}\sinh(J_1\nabla_y)]^4[\cosh(J_2\nabla_y) + m_{zA}\sinh(J_2\nabla_y)]^4 f_\alpha(y)|_{y=0}, \tag{13}$$

where the sublattice magnetizations per site $m_{\alpha\nu}$ $(\nu = A,B)$ are defined by

$$m_{\alpha A} \equiv \langle S_{i\alpha}^A\rangle, \quad m_{\alpha B} \equiv \langle S_{i\alpha}^B\rangle. \tag{14}$$

Then, using the fact that at zero longitudinal magnetic field we have $m_z \equiv m_{zA} = -m_{zB}$ and $m_x \equiv m_{xA}$, one obtains the following equations for the magnetizations, m_α:

$$m_z = \sum_{n=0}^{3} K_{2n+1} m_z^{2n+1}, \tag{15}$$

$$m_x = \sum_{n=0}^{4} K_{2n} m_z^{2n}, \tag{16}$$

where the coefficients K_r $(r = 0,1,\ldots,8)$, which depend on T and R, and Ω, are defined in the Appendix. We note that in obtaining Eqs. (15) and (16) we have made use of the fact that $f_z(y) = -f_z(-y)$ and $f_x(y) = f_x(-y)$ and therefore only odd or even differential operator functions give nonzero contributions, respectively. The expression (15) will be the starting point used here to calculate phase diagrams of the frustrated spin-$\frac{1}{2}$ Ising AF on a square lattice in a transverse field.

III. PHASE DIAGRAM

Now we determine the phase diagram (transition temperature and TCP) between the AF and P phases of the system as follows. In the neighborhood of a second-order transition line where m_z is small, Eq. (15) can be written as

$$m_z = K_1 m_z + K_3 m_z^3 + \cdots. \tag{17}$$

The second-order phase transition line is then determined by

$$K_1 = 1, \quad K_3 < 0. \tag{18}$$

One can note that it is not possible to calculate first-order transition lines on the basis of the equation of state (15) alone because in this case one has $m_z \neq 0$ at the transition point. To solve this problem one needs to compute the free energies for the AF and P phases. First-order transitions correspond then to the locus on the phase diagram where the free energies are equal. Although the EFT does not furnish a way to get such a function, we can resort to a different procedure based on the well-known Landau expansion. In this case we shall extrapolate the free energy based on the relation for the equilibrium magnetization (15) in the following form (see, e.g., Refs. [17,25]):

$$F(T,R,\Omega,m_{za}) = F_0(T,R,\Omega) + \frac{1}{2}\left(1 - \sum_{n=0}^{3}\frac{K_{2n+1}}{n+1} m_{za}^{2n}\right) m_{za}^2, \tag{19}$$

where $F_0(T,R,\Omega)$ is the free energy of the P phase and m_{za} is the order parameter which takes the value m_z at a thermodynamic equilibrium. Indeed, using the equilibrium condition

$$\left.\frac{\partial F(T,R,\Omega,m_{za})}{\partial m_{za}}\right|_{m_{za}=m_z} = 0, \tag{20}$$

we recover Eq. (15) for the equilibrium magnetization m_z. In this way, the second-order phase transition line and a tricritical point, at which the phase transition changes from second order to first order, are determined by the following conditions: (i) the second-order transition line when $1 - K_1 = 0$ and $K_3 < 0$, and (ii) the tricritical point (TCP) when $1 - K_1 = 0$, $K_3 = 0$, if $K_5 < 0$. However, the first-order phase transition line is evaluated by solving simultaneously two transcendental equations, the equilibrium condition (20) and the equation $F(T,R,\Omega,m_{za}) = F_0(T,R,\Omega)$, namely,

$$\sum_{n=0}^{3}\frac{K_{2n+1}}{n+1} m_{za}^{2n} = 1, \tag{21}$$

which corresponds to the point of intersection of the free energies for the AF and P phases. It is worth noticing that for a second-order transition where $m_{za} = 0$ equation the above is the same as Eq. (18), which justifies our procedure. We also note that a similar methodology of obtaining the free energy of the model within the effective-field theory has been proposed in Ref. [26] and used recently to investigate phase diagram of the frustrated Ising [16] and Heisenberg models [27].

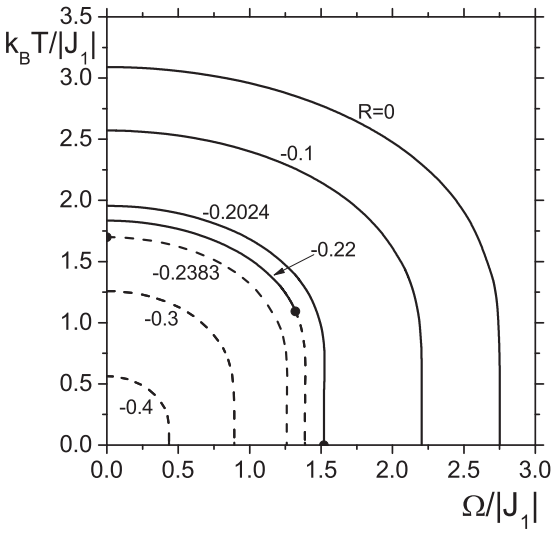

FIG. 3. The transition temperature for the $J_1 - J_2$ Ising model on the square lattice based on the single-spin cluster is plotted as a function of transverse field $\Omega/|J_1|$, for selected values of frustration parameter R. Solid and dashed lines indicate second- and first-order transitions, respectively, while the black circles denote the position of a tricritical point.

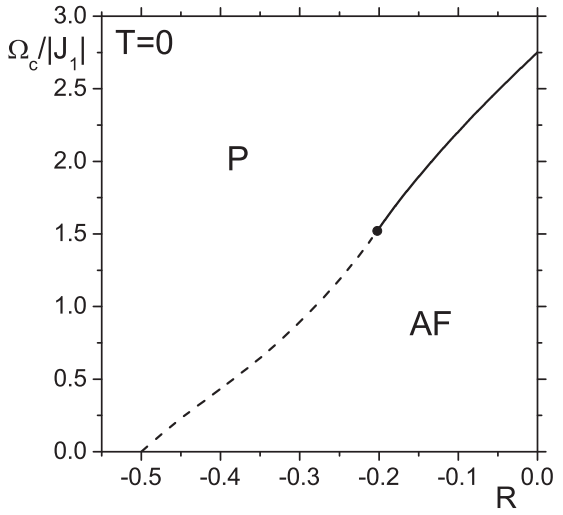

FIG. 4. The dependence of the critical transverse field $\Omega_c/|J_1|$ on the frustration parameter R in the case of $T = 0$. Solid and dashed lines indicate second- and first-order transitions, respectively, while the black circle denotes the position of a tricritical point.

IV. NUMERICAL RESULTS AND DISCUSSION

Now, by using the formulation given in the previous section, let us examine the phase diagrams of the frustrated spin-$\frac{1}{2}$ Ising AF on a square lattice in a transverse field. In all the presented phase diagrams, the solid and dashed lines indicate the second- and first-order phase transitions, respectively, while the black circles denote the positions of TCPs at which phase transitions change from second to first order.

In Fig. 2, the phase diagram $k_BT/|J_1|$ versus R is shown for selected values of $\Omega/|J_1|$. The most important feature in Fig. 2 is that, for $\Omega/|J_1| = 0$, the first-order transition line between the AF and P phases approaches zero when $R = -0.5$, in agreement with the ground-state result. Note that in this case the coordinates of the TCP $(k_BT_t/|J_1|; R_t)$ are (1.7002; -0.2383). For the nonfrustrated model ($R = 0$) and $\Omega/|J_1| = 0$, the critical (or Néel) temperature can be determined from the conditions (18) analytically. In this case, the equation $K_1^{AF} = 1$ reduces to

$$e^{12\beta_N|J_1|} - 3e^{8\beta_N|J_1|} - e^{4\beta_N|J_1|} - 5 = 0 \tag{22}$$

with the solution

$$\frac{k_BT_N}{|J_1|} = \frac{4}{\ln\left[1 + \left(\frac{2}{3}\right)^{2/3}\left(\sqrt[3]{9+\sqrt{69}} + \sqrt[3]{9-\sqrt{69}}\right)\right]}, \tag{23}$$

i.e., $k_BT_N/|J_1| \approx 3.0898$, which can be compared with the exact value of $k_BT_N/|J_1| = 2.2692$ [28]. Further, it can be seen from Fig. 2 that if the value of the transverse field $\Omega/|J_1|$ increases, the TCPs shift towards lower temperatures and for $\Omega/|J_1| = 1.5203$ the TCP vanishes at $R = -0.2024$. It means that for $\Omega/|J_1| > 1.5203$ there is only a second-order transition line between the AF and P phases.

As already mentioned, when Ω increases from zero, the transition temperature falls from its value in the Ising model and reaches zero at a critical value Ω_c (see Fig. 3). The second-order transition is determined from Eq. (18) which for $R = 0$ yields $\Omega_c/|J_1| \approx 2.7510$ and its exact analytical form is given by the expression

$$\frac{\Omega_c}{|J_1|} = \left[2\left(-3 + \sqrt{7 + \sqrt[3]{207 - 48\sqrt{3}} + \sqrt[3]{207 + 48\sqrt{3}}}\right.\right. + \left(14 - \sqrt[3]{207 - 48\sqrt{3}} - \sqrt[3]{207 + 48\sqrt{3}}\right. + \left.\left.\left.\frac{16}{\sqrt{7 + \sqrt[3]{207 - 48\sqrt{3}} + \sqrt[3]{207 + 48\sqrt{3}}}}\right)^{1/2}\right)\right]^{1/2}. \tag{24}$$

As has been discussed in a series of works [28–33], the present EFT based on the approximate relation (3) is expected to give fairly good results for the values of $\Omega/|J_1|$ less than $\Omega_c/|J_1|$. From detailed numerical investigations we have found that for $-0.2024 < R \leqslant 0$ all the critical lines are of second-order phase transitions, while the TCPs appear when $-0.2383 \leqslant R \leqslant -0.2024$. Thus, in the region $-0.5 \leqslant R < -0.2383$ all the transition lines are of first order. This behavior is also clearly seen from Fig. 4 where $\Omega_c/|J_1|$ versus R is shown at the ground state, i.e., at $T = 0$ (see also curves labeled 1.5203 and -0.2024 in Figs. 2 and 3, respectively).

Alternatively, one can study the variation of the TCP (or tricritical temperature T_t) with R_t and $\Omega_t/|J_1|$ in the three-dimensional (3D) space. The results are shown in Fig. 5 by the black curve. The projections of this curve on the $T_t - R_t$, $T_t - \Omega_t$, and $\Omega_t - R_t$ planes (red curves) are also presented.

In order to confirm the prediction of the first- and second-order phase transitions, let us investigate the thermal variations of the longitudinal and transverse magnetizations by solving Eqs. (15) and (16) numerically. The results are depicted in Fig. 6 for the system with $R = -0.22$, when the values of

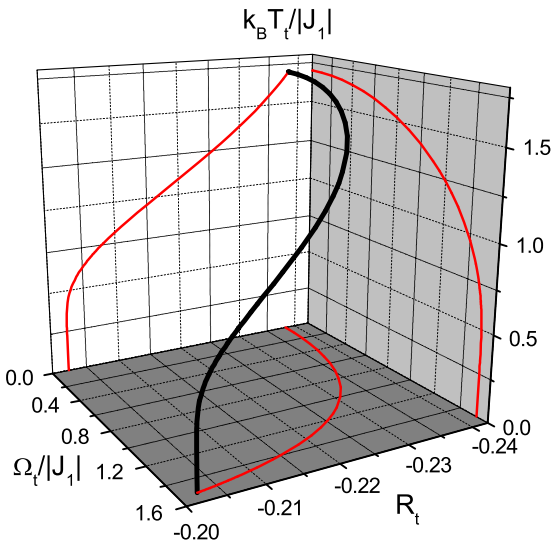

FIG. 5. The dependence of the tricritical temperature T_t on the R_t and $\Omega_t/|J_1|$ in the 3D space (black curve) for the $J_1 - J_2$ Ising model on the square lattice. The red curves indicate its projections on the $T_t - R_t$, $T_t - \Omega_t$, and $\Omega_t - R_t$ planes.

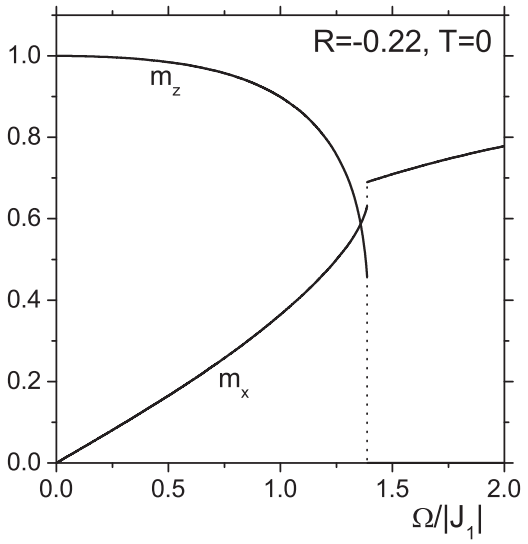

FIG. 7. The dependences of the longitudinal magnetization m_z and transverse magnetization m_x on the transverse field $\Omega/|J_1|$ for the $J_1 - J_2$ Ising model on the square lattice in the case of $R = -0.22$ and $T = 0$. The dotted lines indicate the first-order transitions.

$\Omega/|J_1|$ are changed. As shown in Fig. 6(a), when $\Omega/|J_1| = 1.0$, the longitudinal magnetization m_z shows normal thermal-variation behavior and vanishes at the second-order transition point. Similarly, the m_z also reduced to zero continuously at the TCP (see curve labeled 1.3213). On the other hand, below the TCP, the stable solution of m_z becomes discontinuous at the first-order phase transition and this discontinuity increases from zero to the value of 0.4573 with $\Omega/|J_1|$ going to the $\Omega_c/|J_1| = 1.3872$. The curves for $\Omega/|J_1| = 1.36$ and $\Omega/|J_1| = 1.38$ are examples of such behavior, where the first-order transition is indicated by a vertical dotted line. Further, it is generally seen from Fig. 6(a), that the greater is the transverse field the smaller is the longitudinal magnetization at zero temperature. Thus, the transverse field essentially inhibits the ordering of the S_z component. In contrast, the transverse magnetization [Fig. 6(b)] increases with the transverse field at $T = 0$ and only a weakly depends on temperature in the low-temperature region. Then, after rising rapidly, it passes through a cusp at the second-order transition temperature of m_z before falling off. However, below the TCP, the m_x curves also exhibit discontinuity at the first-order transition temperature of m_z. This discontinuity has a maximum value $\triangle m_x = 0.0591$ at $\Omega_c/|J_1| = 1.3872$ for $T = 0$. As seen from Fig. 7, the discontinuity of m_z is much larger than that of m_x.

V. CONCLUSIONS

In conclusion, the role of the transverse field in the phase transitions of the frustrated $J_1 - J_2$ model on the square lattice is investigated using an EFT. The method is here used in its

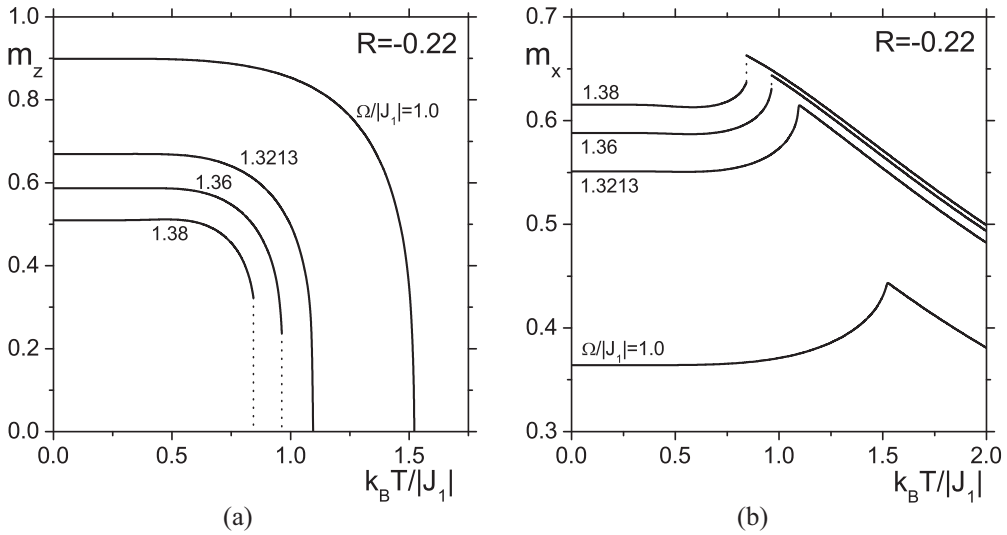

FIG. 6. Temperature dependences of the magnetizations of m_z in (a) and m_x in (b) for the $J_1 - J_2$ Ising model on the square lattice for $R = -0.22$, when values of the transverse field $\Omega/|J_1|$ are changed. The dotted lines indicate the first-order transitions.

simplest approximation version, in which correlations between different spins are neglected. Within this framework we have shown that the transverse field can drastically change the phase diagram of the frustrated $J_1 - J_2$ model on the square lattice. Indeed, we have found that the existence of the TCP in the phase diagram, at which phase transition changes from second to first order, strongly depends on the value of the transverse field Ω. In particular, to analyze the first-order transition between the AF and P phases we proposed the free energy expression. To the best of our knowledge this is the first time that the free energy is developed for the Ising model in a transverse field within the frame of the present EFT. Of course, the reliability on this result could be further increased by using other methods that provide a treatment beyond the effective-field framework. This is, however, a difficult task since frustrated systems are less amenable to numerical and analytical treatments. Even the present relatively simple model in zero field has been approached using various techniques over several decades but its critical behavior remained ambiguous until recently [12,18–20].

Finally, we note that in this paper we focused on the AF phase for $R > -1/2$. However, to investigate effects of the transverse field on the SAF phase, which exists for $R < -1/2$, one needs to consider larger clusters than the single-spin one. In the particular case of the square lattice, the smallest cluster that contains the information on the lattice topology is at least a square cluster (see, e.g., Ref. [17]). This is beyond the scope of the present work and it is an interesting direction for the future research.

ACKNOWLEDGMENTS

This work was supported by the Scientific Grant Agency of Ministry of Education of Slovak Republic (VEGA Nos. 1/0331/15 and 2/0065/17) and the scientific grant of Slovak Research and Development Agency provided under Contract No. APVV-16-0186.

APPENDIX

The coefficients K_r $(r = 0,1,\ldots,8)$ in Eqs. (15) and (16) are defined as follows:

$$K_0 = A_1^4 A_2^4 f_x(y)|_{y=0}, \tag{A1}$$

$$K_1 = 4A_1^3 A_2^3 (A_1 B_2 - A_2 B_1) f_z(y)|_{y=0}, \tag{A2}$$

$$K_2 = A_1^2 A_2^2 [6(A_1 B_2 - A_2 B_1)^2 - 4A_1 A_2 B_1 B_2] f_x(y)|_{y=0}, \tag{A3}$$

$$K_3 = 4A_1 A_2 (A_1 B_2 - A_2 B_1)[(A_1 B_2 - A_2 B_1)^2 - 3A_1 A_2 B_1 B_2] f_z(y)|_{y=0}, \tag{A4}$$

$$K_4 = \left[6A_1^2 A_2^2 B_1^2 B_2^2 - 12A_1 A_2 B_1 B_2 (A_1 B_2 - A_2 B_1)^2 + (A_1 B_2 - A_2 B_1)^4\right] f_x(y)\big|_{y=0}, \tag{A5}$$

$$K_5 = -4B_1 B_2 (A_1 B_2 - A_2 B_1)[(A_1 B_2 - A_2 B_1)^2 - 3A_1 A_2 B_1 B_2] f_z(y)|_{y=0}, \tag{A6}$$

$$K_6 = B_1^2 B_2^2 [6(A_1 B_2 - A_2 B_1)^2 - 4A_1 A_2 B_1 B_2] f_x(y)|_{y=0}, \tag{A7}$$

$$K_7 = -4B_1^3 B_2^3 (A_1 B_2 - A_2 B_1) f_z(y)|_{y=0}, \tag{A8}$$

$$K_8 = B_1^4 B_2^4 f_x(y)|_{y=0}, \tag{A9}$$

where $A_\mu = \cosh(J_\mu \nabla_y)$, $B_\mu = \sinh(J_\mu \nabla_y)$ $(\mu = 1,2)$, and functions $f_\alpha(y)$ $(\alpha = z,x)$ are defined by Eqs. (10) and (11). The coefficients (A1)–(A9) can easily be calculated within the symbolic programming by using the mathematical relation $\exp(\lambda \nabla_y) f_\alpha(y) = f_\alpha(y + \lambda)$, where $\nabla_y = \partial/\partial y$ is a differential operator.

[1] P. de Gennes, Solid State Commun. **1**, 132 (1963).
[2] *Fundamental Problems in Statistical Mechanics II*, edited by E. G. D. Cohen (North-Holland Publishing Co., Amsterdam, 1968).
[3] S. Katsura, Phys. Rev. **127**, 1508 (1968).
[4] P. Pfeuty, Ann. Phys. (NY) **57**, 79 (1970).
[5] M. Suzuki, Phys. Lett. A **34**, 94 (1971).
[6] R. B. Stinchcombe, J. Phys. C **6**, 2459 (1973).
[7] *Introduction to Frustrated Magnetism*, edited by C. Lacroix, P. Mendels, and F. Mila (Springer Verlag, Heidelberg, 2011).
[8] G. H. Wannier, Phys. Rev. **79**, 357 (1950).
[9] R. M. F. Houtapple, Physica **16**, 425 (1950).
[10] J. Villain, J. Phys. C **10**, 1717 (1977).
[11] K. Binder and D. P. Landau, Phys. Rev. B **21**, 1941 (1980).
[12] A. Kalz, A. Honecker, S. Fuchs, and T. Pruschke, Eur. Phys. J. B **65**, 533 (2008).
[13] C. Fan and F. Y. Wu, Phys. Rev. **179**, 560 (1969).
[14] J. L. Morán-López, F. Aguilera-Granja, and J. M. Sanchez, Phys. Rev. B **48**, 3519 (1993).
[15] J. L. Morán-López, F. Aguilera-Granja, and J. M. Sanchez, J. Phys.: Condens. Matter **6**, 9759 (1994).
[16] R. A. dos Anjos, J. R. Viana, and J. R. de Sousa, Phys. Lett. A **372**, 1180 (2008).
[17] A. Bobák, T. Lučivjanský, M. Borovský, and M. Žukovič, Phys. Rev. E **91**, 032145 (2015).
[18] A. Kalz, A. Honecker, and M. Moliner, Phys. Rev. B **84**, 174407 (2011).
[19] S. Jin, A. Sen, and A. W. Sandvik, Phys. Rev. Lett. **108**, 045702 (2012).
[20] S. Jin, A. Sen, W. Guo, and A. W. Sandvik, Phys. Rev. B **87**, 144406 (2013).
[21] F. C. Sá Barreto and I. P. Fittipaldi, Physica A (Amsterdam) **129**, 360 (1985).
[22] H. B. Callen, Phys. Lett. **4**, 161 (1963).
[23] M. Suzuki, Phys. Lett. **19**, 267 (1965).
[24] R. Honmura and T. Kaneyoshi, J. Phys. C **12**, 3979 (1979).

[25] A. Bobák, M. Tóthová, and T. Balcerzak, J. Magn. Magn. Mater. **128**, 29 (1993).
[26] R. A. dos Anjos, J. R. Viana, J. R. de Sousa, and J. A. Plascak, Phys. Rev. E **76**, 022103 (2007).
[27] R. S. Lapa, G. Mendonça, J. R. Viana, and J. R. de Sousa, J. Magn. Magn. Mater. **369**, 44 (2014).
[28] L. Onsager, Phys. Rev. **65**, 117 (1944).
[29] E. F. Sarmento, I. Tamura, L. E. M. C. de Oliviera, and T. Kaneyoshi, J. Phys. C **17**, 3195 (1984).
[30] I. Tamura, E. F. Sarmento, and T. Kaneyoshi, J. Phys. C **17**, 3207 (1984).
[31] T. Kaneyoshi, J. Phys. Soc. Jpn. **54**, 3514 (1985).
[32] T. Kaneyoshi, J. Phys. C **19**, 2979 (1986).
[33] T. Kaneyoshi, Phys. Rev. B **33**, 526 (1986).